of the result of the thin-layer coulometry, the number of electrons concerned with reduction and oxidation is 1. These results indicate that the cluster **3** undergoes one-electron reversible reduction and one-electron reversible oxidation in dichloromethane. The voltammetric behavior of **3** in THF is very similar to that in dichloromethane. Accordingly, the electrochemical processes are expressed as

$$[W_6S_8(PEt_3)_6]^+ \underset{-e^-}{\overset{+e^-}{\rightleftharpoons}} [W_6S_8(PEt_3)_6] \underset{-e^-}{\overset{+e^-}{\rightleftharpoons}} [W_6S_8(PEt_3)_6]^-$$

The formal potentials for **3** vs the Fc/Fc^+ redox couple are given in Table V.

Discussion

Synthesis. As the intermediate trinuclear complex has not been fully characterized and the yield of the hexanuclear complex **3** is rather low, the pathway of the formation of **3** is not clear at present. However, it is likely that the hexanuclear cluster complex is formed by reductive dimerization of two trinuclear cluster complexes.[2]

Structure. The cluster complex **3** is the first example of a compound with the W_6S_8 cluster framework. Neither solid compounds nor molecular complexes with this cluster unit are known,[11] but the structural features of **3** are almost identical with those of the molybdenum analogue.[2] Just like the molybdenum complex, the 20-electron tungsten cluster complex is free from strong intercluster interactions and has a regular octahedral cluster skeleton. Although the molecular orbital calculation of the W_6S_8 clusters has not been reported, the basic level scheme should be similar to that of the Mo_6S_8 clusters;[12] namely, the HOMO is either the triply degenerate t_{2u} or t_{1u} and the LUMO is doubly degenerate e_g. The undistorted octahedron of the cluster implies that the HOMO is just occupied with 20 electrons.

The W-W bond distance (average) of 2.678 Å in **3** is slightly longer than that in the 24e cluster complex $[W_6Cl_{12}(PBu_3)_2]$ (**5**) (average) of 2.626 Å.[13] The longer distance can be interpreted in terms of a larger electrostatic repulsion between the tungsten atoms in the 16/6 oxidation state as compared with 12/6 in **5**. The average W-W bond distance in **3** is slightly longer than the Mo-Mo distance in the molybdenum analogue **4** (2.663 Å). A similar trend has been observed in the 24e cluster complexes $[M_6Cl_{12}(PBu_3)_2]$ (M = Mo, W).[13,14]

Orbital Energy Levels and Electron Transfer. Although the whole structure is almost identical with that of the molybdenum analogue, the tungsten cluster is significantly different in the electronic properties. The electrochemical reduction and oxidation potentials of the compound are related to the LUMO and HOMO energy levels, respectively.[15] The energy difference of the cathodic and anodic processes approximates the energy difference of the frontier orbitals. The energy difference is 1.37 eV for the dichloromethane solution and 1.52 eV for the THF solution of the cluster **3**. Corresponding values for the molybdenum cluster are 1.27 and 1.45 eV. Therefore, the energy differences for the tungsten cluster **3** are about 0.1 eV larger in both solvents. The main bands of the electronic spectra at longer wavelengths (882 nm (1.40 eV) for **3** and 991 nm (1.25 eV) for **4**)[2] are probably the transitions between the HOMO and LUMO. The values are near those of the electrochemistry in dichloromethane. The nature of the solvent effects is not clear at present. The molecular orbital calculations for the Mo_6S_8 systems have shown that the energy difference between the HOMO (t_{2u} or t_{1u}) and the LUMO (e_g) is about 1 eV.[12] As the redox potentials should reflect the involved orbital energies, the frontier orbitals of the tungsten complex are at a level about 0.2-0.3 eV higher than those of the molybdenum analogue. This energy difference in the molecular clusters $[M_6S_8(PEt_3)_6]$ (M = Mo, W) would also remain in the solid-state M_6S_8 compounds and affect the conductivity properties. We anticipate the synthesis of the solid-state tungsten cluster compounds with W_6S_8 cluster units.

Acknowledgment. The support from the Ministry of Education, Science and Culture of Japan (Grant-in-Aid for General Research No. 63430010) and the gift of triethylphosphine from Nippon Chemical Co. Ltd. are gratefully acknowledged. The XPS spectra were measured at the Coordination Chemistry Laboratories of the Institute for Molecular Science under the Cooperative Research Program.

Supplementary Material Available: Listings of anisotropic thermal parameters, powder diffraction data for **2**, and complete crystal data for **3** (4 pages); a listing of calculated and observed structure factors for **3** (14 pages). Ordering information is given on any current masthead page.

(11) Yvon, K. In ref 1, p 90.
(12) (a) Le Beuze, L.; Makhyoun, M. A.; Lissillour, R.; Chermette, H. *J. Chem. Phys.* **1982**, *76*, 6060. (b) Hughbanks, T.; Hoffmann, R. *J. Am. Chem. Soc.* **1983**, *105*, 1150. (c) Burdett, J. K.; Lin, J. H. *Inorg. Chem.* **1982**, *21*, 5. (d) Imoto, H.; Saito, T.; Adachi, H. To be submitted for publication.
(13) Saito, T.; Manabe, H.; Yamagata, T.; Imoto, H. *Inorg. Chem.* **1987**, *26*, 1362.
(14) Saito, T.; Nishida, M.; Yamagata, T.; Yamagata, Y.; Yamaguchi, Y. *Inorg. Chem.* **1986**, *25*, 1111.
(15) Lemoine, P. *Coord. Chem. Rev.* **1988**, *83*, 169.

Contribution from the Institute of Inorganic Synthesis, Yamanashi University, Miyamae-cho 7, Kofu 400, Japan

A New Lithium Insertion Compound, $(Li,Cu)TaO_3$, with the $LiNbO_3$ Type Structure

Nobuhiro Kumada,* Satoru Hosoda, Fumio Muto, and Nobukazu Kinomura

Received November 28, 1988

A new lithium insertion compound, $(Li,Cu)TaO_3$, was prepared from $CuTa_2O_6$ by chemical reaction with *n*-butyllithium. The lithium insertion reaction was accompanied by a topotactic transformation from the perovskite-related structure to the $LiNbO_3$ type structure. The hexagonal lattice parameters of the compound are $a = 5.176$ (2) and $c = 13.81$ (1) Å. The structure was refined by the X-ray powder Rietveld method; reliability factors are $R_{wP} = 5.7$, $R_P = 4.5$, and $R_B = 7.4\%$. The cation arrangement of $(Li,Cu)TaO_3$ is similar to that of $LiTaO_3$ rather than to that of the high-pressure form of $CuTaO_3$.

Introduction

Lithium insertion (lithiation) has been investigated on various transition-metal oxides by chemical or electrochemical methods. Lithiation is an important secondary battery cathode reaction and has been extended to syntheses of new compounds, as seen, for example, in the lithiation of ReO_3,[1] rutile,[2] and spinel[3-5] type oxides. These oxides have cavities or tunnels available to incorporate the lithium ions. In many cases the oxygen array of

(1) Cava, R. J.; Santoro, A.; Murphy, D. W.; Zahurak, S.; Roth, R. S. *J. Solid State Chem.* **1982**, *42*, 251.
(2) Murphy, D. W.; Di Salvo, F. J.; Waszczak, J. N. *Mater. Res. Bull.* **1978**, *13*, 1395.
(3) Chen, C. J.; Greenblatt, M. *Solid State Ionics* **1986**, *18&19*, 838.
(4) Chen, C. J.; Greenblatt, M.; Waszczak, J. V. *J. Solid State Chem.* **1986**, *64*, 240.
(5) Thackeray, M. M.; David, W. I. F.; Bruce, P. G.; Goodenough, J. B. *Mater. Res. Bull.* **1983**, *18*, 461.

0020-1669/89/1328-3592$01.50/0

a host lattice remains intact during lithiation. However, the cubic close-packed oxygen array of ReO_3 was reported to transform dramatically to the hexagonal one upon lithiation.[1] A reverse topotactic transformation was observed in the proton-exchange reaction of $LiMO_3$ (M = Nb, Ta) to give perovskite type HMO_3.[6] These structural changes are rather exceptional in the so-called "soft chemistry" such as lithiation, intercalation, and ion exchange.

There had been several arguments on the crystal structure of $CuTa_2O_6$,[7-10] but finally Vincent et al. solved the structure by using a single crystal.[11] They report for this compound a pseudocubic orthorhombic system with cell parameters a = 7.5228 (9), b = 7.5248 (9), and c = 7.5199 (9) Å and a perovskite type framework built up from the corner sharing of TaO_6 octahedra. Copper ions are located at the nearly square-planar site in the cavities unlike the large cation in the ideal perovskite type structure.

We describe here preparation of the lithium insertion compound (Li,Cu)TaO_3 from $CuTa_2O_6$ and its properties and compare its structure with those of other $LiNbO_3$ type compounds.

Experimental Section

A starting powder of $CuTa_2O_6$ was synthesized as reported previously.[7] Lithiation was carried out by stirring the starting powder (2 g) in a 0.08 M hexane solution of *n*-butyllithium. The reaction temperature was 50 °C, and the duration time ranged from 1 to 7 days. Solid products were separated by centrifugation, washed well with hexane, and then dried under vacuum at room temperature. A small amount of white impurity thought to be hydrolysis products of *n*-butyllithium was observed in the samples. It was dissolved with distilled water. The lithium and copper content was determined by atomic absorption spectroscopy. Magnetic susceptibility was measured with the Faraday method over the temperature range from liquid-nitrogen temperature to 480 K.

Products were identified by X-ray powder diffractometry with Ni-filtered Cu Kα radiation. Lattice parameters were determined by least-squares refinement of powder data taken with a scanning speed of $^1/_4$°/min. Silicon was used as an internal standard with the cell parameter a = 5.4301 Å. The crystal structure was refined with the X-ray powder Rietveld method.[12] Intensity data were collected by using Ni-filtered Cu Kα radiation for 10 s at 0.05° intervals over 2θ angles from 10 to 100°.

Results and Discussion

1. Lithium Insertion into $CuTa_2O_6$. The X-ray powder pattern of the prepared powder was indexed with the pseudocubic system, similar to that of previous studies. Although on lithiation the sample changed to black in several hours, more than 2 days were necessary to obtain the single-phase product. When the reaction time was less than 2 days, a small amount of the starting compound remained.

The X-ray powder pattern of the product was similar to those of $LiMO_3$ (M = Nb, Ta)[13] and could be indexed completely with a hexagonal cell of a = 5.176 (2) and c = 13.81 (1) Å. The composition of the product was determined to be $Li_{1.2}Cu_{0.8}Ta_2O_6$ by chemical analysis (Anal. Found: Li, 1.6 ± 0.1; Cu, 10.5 ± 0.8. Calcd: Li, 1.6; Cu, 9.8) and hereafter is denoted as (Li,Cu)TaO_3 because, as is mentioned later, Li and Cu ions randomly occupy the same crystallographic site in the $LiNbO_3$ type structure. The Li/Cu ratio of the products was independent of lithiation conditions. The specific gravity measured with a pycnometer was 8.21 g/cm^3, in good agreement with the calculated value (8.20 g/cm^3).

The composition $Li_{1.2}Cu_{0.8}Ta_2O_6$ implies that copper ions are partially replaced by lithium ions during lithiation. It is likely that the removed Cu^+ ions are reduced to Cu^0 in the reducing nonaqueous solution and that the Cu^0 is adsorbed by parent particles and finally washed off. Similar extraction of the transition metal from the parent lattice was observed in the excess lithiation of Fe_3O_4 and Fe_2O_3.[14] The partial replacement of copper ions with lithium ions up to 3/2 of the ratio Li/Cu may be correlated with the low solubility of copper in the solid solution of $Li_{1-x}Cu_xTa_{1-x}Ti_xO_3$ (x = 0.25) with the $LiNbO_3$ type structure prepared at high temperatures.[15]

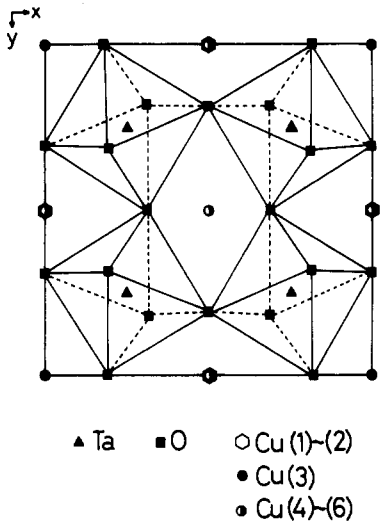

Figure 1. Crystal structure of $CuTa_2O_6$, viewed down the c axis. Cu(1-3) are located in the middle of the pseudocubic edges, and Cu(4-6) are statistically distributed over the face centers.

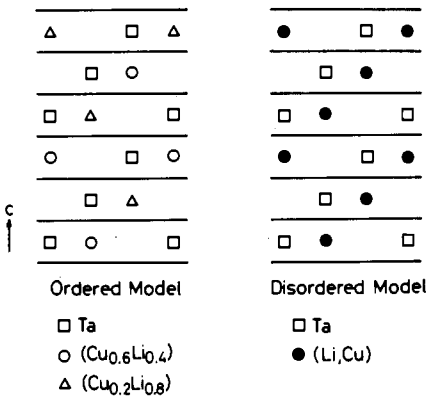

Figure 2. Ordered and disordered models of (Li,Cu)TaO_3. Full lines denote the hexagonal close-packed oxygen array.

2. Properties of $CuTa_2O_6$ and (Li,Cu)TaO_3. A linear relationship between $1/\chi_m$ and T was observed over the measured temperature range, thus showing that the Curie–Weiss law was obeyed. We did not observe two linear regions as indicated by Longo and Sleight.[7] The effective magnetic moment, μ_{eff}, and paramagnetic Curie temperature, θ_p, were calculated to be 2.0 μ_B and −27 K, respectively. These values agree with those of 2.06 μ_B and −15 K, respectively, reported by Krylov et al.[16] The μ_{eff} values are significantly larger than the calculated spin-only value of 1.73 μ_B for Cu^{2+}. The difference is probably due to the spin–orbital interaction, as mentioned by Krylov et al.

(Li,Cu)TaO_3 exhibited diamagnetism over the temperature range from liquid-nitrogen temperature to room temperature. This result implies absence of atoms having any magnetic moment and thus supports neither existence of Cu^{2+} ions nor reduction of Ta^{5+} ions in the product. Electrical resistances for both compounds measured on pelletized samples were too high to be detectable.

3. Structural Consideration of the Product. In order to confirm the $LiNbO_3$ type structure for (Li,Cu)TaO_3, structure refinements were carried out by the Rietveld method. In Figure 1 the structure

(6) Rice, C. E.; Jackel, J. L. *J. Solid State Chem.* **1982**, *41*, 308.
(7) Longo, J. M.; Sleight, A. W. *Mater. Res. Bull.* **1975**, *10*, 1273.
(8) Kasper, H. *Rev. Chim. Miner.* **1967**, *4*, 759.
(9) Reinen, D.; Propach, V. *Inorg. Nucl. Chem. Lett.* **1971**, *7*, 569.
(10) Goodenough, J. B.; Hong, H. Y. P.; Kafalas, J. A. *Mater. Res. Bull.* **1976**, *11*, 203.
(11) Vincent, H.; Bochu, B.; Aubert, J. J.; Joubert, J. C.; Marezio, M. *J. Solid State Chem.* **1978**, *24*, 245.
(12) Izumi, F. *J. Miner. Soc. Jpn.* **1985**, *17*, 37.
(13) Megaw, H. D. *Acta Crystallogr.* **1968**, *A24*, 583.
(14) Thackeray, M. M.; David, W. I. F.; Goodenough, J. B. *Mater. Res. Bull.* **1982**, *17*, 785.
(15) Mouron, P.; Choisnet, J. *J. Phys. Colloq. Cl* **1986**, *47*, 491.
(16) Krylov, E. I.; Bazeuv, G. V.; Vhan, V. P. *Izv. Akad. Nauk SSSR, Neorg. Mater.* **1969**, *5*, 2029.

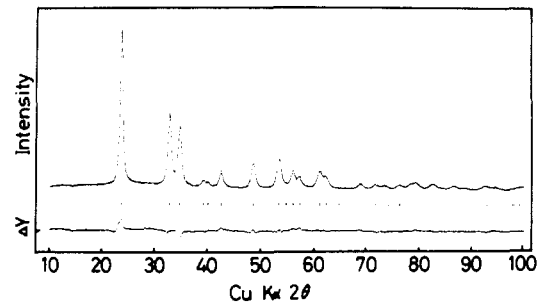

Figure 3. Rietveld refinement pattern for $(Li,Cu)TaO_3$. Observed data are denoted by dots, and the calculated pattern is drawn by the solid line in the upper part. Positions of reflections calculated for Cu $K\alpha_1$ and Cu $K\alpha_2$ are marked by vertical bars in the middle part. The lower portions are plots of ΔY, the differences between observed and calculated intensities.

Table I. Positional and Thermal Parameters for $(Li,Cu)TaO_3$ (Estimated Standard Deviations in Parentheses)

atom	position	x	y	z	B,[a] Å^2
Ta	6a	0	0	0	0.9 (3)
(Li,Cu)	6a	0	0	0.292 (2)	1.6*
O	18b	0.071 (10)	0.354 (20)	0.076 (8)	0.27*

[a] Asterisk denotes a fixed parameter.

of $CuTa_2O_6$ is shown. TaO_6 octahedra form distorted ReO_3 type framework, and Cu^{2+} ions in the cavities have a square-planar coordination with oxygen instead of 12-fold coordination of the large cation in the perovskite type structure. In the structure the sites for the large cation in the perovskite type structure are occupied with Cu^{2+} ions in such a way that the Cu-rich layer and vacancy-rich layer are stacked alternatively along the ⟨111⟩ direction, which corresponds to the c axis of $LiNbO_3$ type structure. Three-fourths of the sites are filled with Cu in the former layer, and one-fourth, in the latter, although Cu^{2+} ions and vacancies are ordered in each layer.

In Figure 2 two models of the (Li,Cu) array along the c axis of the $LiNbO_3$ type structure are shown. The first one is composed of the alternative arrangement Cu-rich layer and Li-rich layer where Li^+ ions are inserted into the vacancies in $CuTa_2O_6$, reflecting the ordered arrangement of Cu^{2+} ions and vacancies in the mother crystal. On the other hand, Li^+ and Cu^+ ions are distributed randomly in the second model. The space group is $R3$ for the ordered model and $R3c$, same as $LiTaO_3$,[17] for the disordered one. Rietveld refinements resulted in the final R factors, R_{wP}, R_P, and R_B, defined in ref 18 of 10.8, 8.1, and 12.6% for the ordered model and 5.7, 4.5, and 7.4% for the disordered one. Absence of the 003 reflection, for example, clearly indicated that the disordered model was most plausible. Therefore, the product can be reasonably represented as $(Li,Cu)TaO_3$. Observed and calculated diffraction patterns for the disordered model are shown in Figure 3, and the atomic parameters are thermal parameters are listed in Table I. In this refinement the modified pseudo-Voigt function was adopted as a profile shape function,[12] and 20 variable parameters were refined. The thermal parameters of (Li,Cu) and oxygen were fixed at 1.6 and 0.27 Å^2, respectively, which were quoted from the thermal parameters for lithium and oxygen in $LiReO_3$;[1] otherwise, the thermal parameter of (Li,Cu) reached a very large value of 12 Å^2. As pointed out by Young and Wiles, thermal parameters in Rietveld refinements are more sensitive to the profile shape function than to positional parameters.[18] The powder pattern of the product was rather broad, and Li is a light element. It is difficult to discuss the meaning of the large thermal parameter, because single-crystal data were not available.

As the product can be regarded to be the solid solution between $LiTaO_3$ and $CuTaO_3$ that was prepared under high pressure,[19]

Table II. Interatomic Distances (Å) and Angles (deg) for $(Li,Cu)TaO_3$

	$(Li,Cu)O_6$ Octahedron		
(Li,Cu)–O	2.15 (7) (×3)	O–O	2.61 (9) (×3)
	2.21 (9) (×3)		2.77 (15) (×3)
	2.18 (av)		3.12 (16) (×3)
			3.54 (17) (×3)
			3.01 (av)
O–(Li,Cu)–O	73.4		
	78.9		
	91.4		
	108.2		
	88.0 (av)		
	TaO_6 Octahedron		
Ta–O	1.96 (9) (×3)	O–O	2.61 (11) (×3)
	1.98 (9) (×3)		2.77 (15) (×3)
	1.97 (av)		2.83 (14) (×3)
			2.91 (12) (×3)
			2.78 (av)
O–Ta–O	82.9		
	89.5		
	92.1		
	95.2		
	89.9 (av)		
	Metal–Metal		
(Li,Cu)–(Li,Cu)	3.77 (2)	Ta–Ta	3.772 (1)
(Li,Cu)–Ta	3.042 (5)		

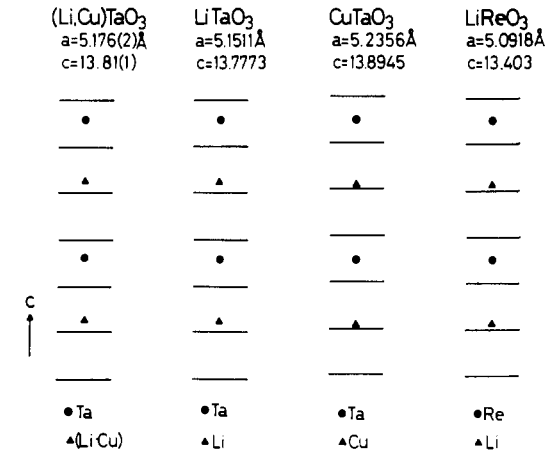

Figure 4. Models of atomic arrangements for $LiNbO_3$ type compounds. Full lines denote the hexagonal close-packed oxygen array.

the lattice parameters of a = 5.176 (2) and c = 13.81 (1) Å for $(Li,Cu)TaO_3$ are intermediate values between those of the two compounds. Calculated interatomic distances and angles are listed in Table II. The mean value of Ta–O distances for $(Li,Cu)TaO_3$, 1.97 Å, is consistent with those of other isostructural tantalates, 1.990 Å for $LiTaO_3$ or 1.987 Å for $CuTaO_3$. The mean value of (Li,Cu)–O distances of the $(Li,Cu)O_6$ octahedron is 2.18 Å, and this value is close to 2.174 Å for the Li–O distance in $LiTaO_3$ but is smaller than 2.410 Å for Cu–O in $CuTaO_3$.

For structural comparison among the $LiNbO_3$ type compounds that are characterized by ferroelectric polarization along the c axis, the crystallographic z parameters of the atoms are used often. The atomic arrangements in $LiTaO_3$, the high-pressure phase of $CuTaO_3$, and lithium insertion compounds $LiReO_3$ and $(Li,Cu)TaO_3$ are schematically shown in Figure 4 after the representation of Abrahams and Bernstein.[20] The displacements of Ta and (Li,Cu) from the oxygen sheet for $(Li,Cu)TaO_3$ are 0.08 and 0.05, respectively. They are close to the values of 0.069 and 0.044 for $LiTaO_3$. In other compounds, the values are 0.087 and 0.006 for $CuTaO_3$ and 0.079 and 0.027 for $LiReO_3$, and the cations in the two compounds are nearer to the oxygen sheet than those of $(Li,Cu)TaO_3$ and $LiTaO_3$. The maximum approach that

(17) Santoro, A.; Roth, R. S.; Austin, A. *Acta Crystallogr.* **1982**, *B38*, 1094.
(18) Young, R. A.; Wiles, D. B. *J. Appl. Crystallogr.* **1982**, *15*, 430.
(19) Sleight, A. W.; Prewitt, C. T. *Mater. Res. Bull.* **1970**, *5*, 207.
(20) Abrahams, S. C.; Bernstein, J. L. *J. Phys. Chem. Solids* **1967**, *28*, 1685.

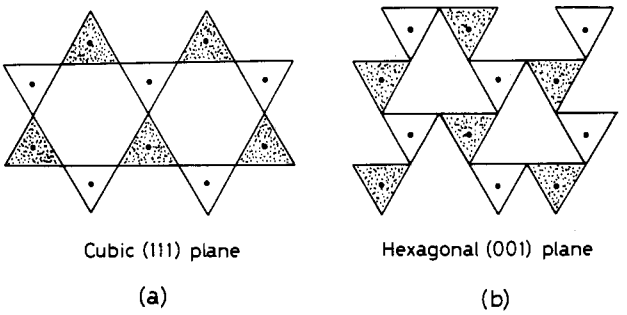

Figure 5. Transformation from the cubic close-packed oxygen array of ReO_3 (a) to the hexagonal close-packed one of $LiReO_3$ (b). Solid circles and triangles show Re ions and triangular faces of the ReO_6 octahedra, respectively. Oxygen ions are placed at the vertices. Triangles of octahedra above the plane of the structure are shaded, and that of octahedra below are unshaded.

is attained by placing the cation in the oxygen sheet is seen in the high-temperature paraelectric form of $LiMO_3$ (M = Nb, Ta).[21] The cation arrangement of $(Li,Cu)TaO_3$ is similar to that of ferroelectric $LiTaO_3$. As the structure of $(Li,Cu)TaO_3$ was refined by using powder data and lithium is a light element, the position of the lithium ions remains somewhat ambiguous. Further investigation of the dielectric property of this compounds is needed.

4. Structural Change from the Perovskite-Related Structure to the $LiNbO_3$ Type Structure. The lithiation of $CuTa_2O_6$ with the perovskite-related structure resulted in the formation of $(Li,Cu)TaO_3$ with the $LiNbO_3$ type structure. Similar structural transformation is observed in lithium insertion into ReO_3 to yield $LiReO_3$ and Li_2ReO_3.[1] In this case, corner-shared ReO_6 octahedra are rotated by approximately 60° around the ⟨111⟩ direction of the cubic system and the rotation axis becomes the hexagonal c axis of the new $LiNbO_3$ type structure as shown in Figure 5.

During this topotactic process, an intermediate phase, $Li_{0.2}ReO_3$, appeared,[22] having the framework significantly distorted from that of the original lattice in a way similar to the distortion reported for $AC_3B_4O_{12}$ (A = Na, Ca, Sr, Ln; B = Ti, Ge, Fe, Nb, Ta, Mn; C = Cu, Mn).[23] Similar distortion has been often observed in the products of "soft chemistry" such as the lithiated compound $Li_{0.36}WO_3$[22] and HMO_3 (M = Nb, Ta), the products of the reverse topotactic reaction mentioned above.[6] Defect perovskites containing large trivalent lanthanide ions $Ln_{1/3}NbO_3$ (Ln = La, Nd) were reported not to undergo this topotactic change on lithiation.[24]

The structural change from the distorted perovskite type to $LiNbO_3$ type structures on the lithiation of $CuTa_2O_6$ can be regarded to be a topotactic one as is the case of the lithiation of ReO_3.[1] The facts that the framework of $CuTa_2O_6$ is already deformed from that of ideal perovskite structure and is similar to that observed for the intermediate phase between the perovskite and $LiNbO_3$ type structures seem to make it facile for the corner-shared octahedra to rotate around the ⟨111⟩ direction.

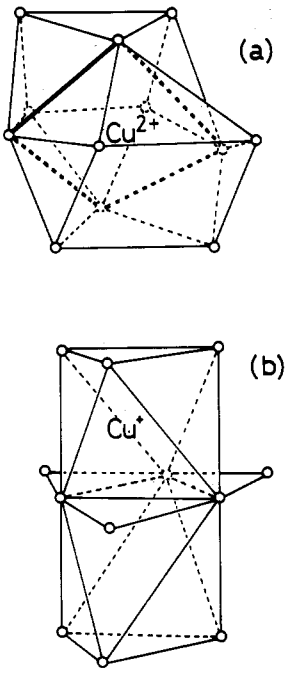

Figure 6. Transformation of the coordination of the Cu ion: (a) square-planar coordination for $CuTa_2O_6$; (b) octahedral coordination for $(Li,Cu)TaO_3$.

The two kinds of cavities in $CuTa_2O_6$, which are filled with the copper ions or are empty, are deformed to produce two octahedral sites linked by face-sharing, as shown in Figure 6, on the structural change. The copper ions reduced to Cu^+ are moved to one of the two octahedral sites, and simultaneously the inserted lithium ions are incorporated at one of two octahedral sites formed from the empty cavity. The octahedral sites filled with the copper and lithium ions are ordered to form the $LiNbO_3$ type structure.

The topotactic reaction on the lithiation of $CuTa_2O_6$ led to the formation of $Li_{1.2}Cu_{0.8}Ta_2O_6$ with the $LiNbO_3$ type structure. It is noteworthy that $(Li,Cu)TaO_3$, which can be regarded as a solid solution between $LiTaO_3$ and $CuTaO_3$, could be prepared from the compound having a structure different from both end members under completely different conditions by means of soft chemistry.

Acknowledgment. This work was supported by the Grant-in-Aid of the Ministry of Education, Science, and Culture of Japan (63750772).

(21) Abrahams, S. C.; Levinstein, H. J.; Reddy, J. M. *Ibid.* **1966**, *27*, 1019.
(22) Cava, R. J.; Santoro, A.; Murphy, D. W.; Zahurak, S. M.; Roth, R. S. *J. Solid State Chem.* **1983**, *50*, 121.
(23) Bochu, B.; Deschizeaux, M. N.; Joubert, J. C.; Collomb, A.; Chenavas, J.; Marezio, M. *J. Solid State Chem.* **1979**, *29*, 291.
(24) Nadiri, A.; Le Flem, G.; Delmas, C. *J. Solid State Chem.* **1988**, *73*, 338.